Structure analysis and site-directed mutagenesis of defined key residues and motives for pilus-related sortase C1 in group B *Streptococcus*

Roberta Cozzi,* Enrico Malito,*,† Annalisa Nuccitelli,* Mariapina D'Onofrio,‡ Manuele Martinelli,* Ilaria Ferlenghi,* Guido Grandi,* John L. Telford,* Domenico Maione,*,[1] and C. Daniela Rinaudo*

*Novartis Vaccines and Diagnostics, Siena, Italy; †Genomics Institute of the Novartis Research Foundation, San Diego, California, USA; and ‡Department of Biotechnology, University of Verona, Verona, Italy

ABSTRACT **In group B *Streptococcus* (GBS), 3 structurally distinct types of pili have been discovered as potential virulence factors and vaccine candidates. The pilus-forming proteins are assembled into high-molecular-weight polymers *via* a transpeptidation mechanism mediated by specific class C sortases. Using a multidisciplinary approach including bioinformatics, structural and biochemical studies, and *in vivo* mutagenesis, we performed a broad characterization of GBS sortase C1 of pilus island 2a. The high-resolution X-ray structure of the enzyme revealed that the active site, into the β-barrel core of the enzyme, is made of the catalytic triad His157-Cys219-Arg228 and covered by a loop, known as the "lid." We show that the catalytic triad and the predicted N- and C-terminal transmembrane regions are required for the enzyme activity. Interestingly, by *in vivo* complementation mutagenesis studies, we found that the deletion of the entire lid loop or mutations in specific lid key residues had no effect on catalytic activity of the enzyme. In addition, kinetic characterizations of recombinant enzymes indicate that the lid mutants can still recognize and cleave the substrate-mimicking peptide at least as well as the wild-type protein.—Cozzi, R., Malito, E., Nuccitelli, A., D'Onofrio, M., Martinelli, M., Ferlenghi, I., Grandi, G., Telford, J. L., Maione, D., Rinaudo, C. D. Structure analysis and site-directed mutagenesis of defined key residues and motives for pilus-related sortase C1 in group B *Streptococcus*. *FASEB J.* 25, 1874–1886 (2011). www.fasebj.org**

Key Words: pilus islands · pilus polymerization · backbone protein · ancillary proteins · in vivo *complementation mutagenesis*

GROUP B *STREPTOCOCCUS* (GBS), known also as *Streptococcus agalactiae*, is the leading cause of neonatal sepsis worldwide (1). In recent years, pili, long filamentous fibers protruding from the bacterial surface, have been identified in GBS, as well as in other gram-positive pathogens, as important virulence factors and potential vaccine candidates (2, 3). Different from the well-known gram-negative pili, gram-positive pili are covalently linked structures, constituted by a major pilin subunit, the backbone protein (BP), associated with the ancillary proteins (4). The current model of pilus biogenesis consists of a biphasic process wherein pilus polymerization is catalyzed by class C pilus-specific sortases *via* a transpeptidation mechanism from backbone and ancillary pilin precursor substrates, followed by cell wall anchoring of the pilus promoted by the housekeeping sortase A (5–7). A C-terminal LPXTG motif (where X represents any amino acid) is present in the structural proteins and is the sortase recognition site typically conserved in cell wall-anchored proteins (4, 8). Class C sortases are integral membrane cysteine transpeptidases of gram-positive bacteria (9). As pilin subunits emerge, sortases cleave the LPXTG motif of the pilin proteins and covalently join the C terminus of one pilin subunit to a Lys side-chain NH_2 group on the next subunit (4–6, 9). In GBS, we have identified 3 pilus variants whose genes coding for the structural proteins and for pilus-related C sortases are present in pathogenicity genomic islands [pilus island (PI)-1, PI-2a, and PI-2b; refs. 10, 11]. Genetic studies previously performed in the PI-2a genomic locus have established the relative contribution of the two pilus-associated sortases, SrtC1 and SrtC2. The enzymes were found to be redundant in terms of their activity on the BP polymerization, since only the deletion of both sortase C genes completely abolished pilus polymerization (11). However, the two SrtC enzymes showed some specificity for the incorporation of the ancillary proteins into pili; SrtC1 was more specific for the pilus linkage of the minor ancillary protein (AP2), and SrtC2 was more specific for the major ancillary protein (AP1). The minor ancillary protein AP2 appears to be the

[1] Correspondence: Novartis Vaccines, Via Fiorentina 1, 53100 Siena, Italy. E-mail: domenico.maione@novartis.com

doi: 10.1096/fj.10-174797

This article includes supplemental data. Please visit *http://www.fasebj.org* to obtain this information.

0892-6638/11/0025-1874 © FASEB

terminal subunit in pilus assembly, identified as the protein that anchors the entire pilus structure to the cell wall (12). Linkage of the assembled pilus *via* AP2 to the cell wall peptoglycan is mediated by the housekeeping sortase A (Srt-A; refs. 12, 13). By contrast, no detectable role in pilus polymerization for the housekeeping SrtA in GBS was found (11, 12).

Recently, an extensive characterization of pilus-associated sortases from *Streptococcus pneumoniae* (SrtC-1, SrtC-2, and SrtC-3) was performed, and the X-ray structures of all 3 SrtC enzymes have been solved (14, 15). The 3-dimensional structures revealed that these enzymes possess a catalytic triad constituted of His, Arg, and Cys within the active substrate recognition region and a mobile lid encapsulating the active site in a closed conformation in the absence of substrate (14, 15). While the catalytic triad of Cys, His, and Arg side chains within the active site cleft is absolutely conserved among different classes of sortases (16, 17), including SrtA from *Staphylococcus aureus*, the region corresponding to the lid is thus far found only in X-ray diffraction-solved crystal structures of pilus-related C sortases in gram-positive bacteria (14, 18).

In the present study, we combine structural analysis, biochemical assays, site-directed mutagenesis, and complementation studies of deletion mutant strains for an extensive characterization of GBS sortase C1 of PI-2a. The crystal structure of the enzyme was solved by X-ray crystallography, and its metal-binding properties were investigated by NMR spectroscopy. Multiple alignments of homologous proteins and structural comparative analysis have been used to predict the specific amino acid residues and regions required for catalytic enzyme activity and specificity in pilus protein polymerization. We show that the SrtC1 amino acids C219, H157, and R228 in the catalytic triad are absolutely required for pilus polymerization, whereas the deletion of the lid region has no effect on pilus polymerization. Finally, the role of the two predicted transmembrane (TM) domains was also explored by deletion of these regions and *in vitro* assays using recombinant proteins and fluorescent peptides.

MATERIALS AND METHODS

Bioinformatics

Prediction of TM helices and membrane topology of sortase protein sequences was obtained using the Analyze and Edit Transmembrane Protein tool of Discovery Studio 2.5 (Accelrys, San Diego, CA, USA). Multiple sequence alignment and phylogenetic analysis were performed using the neighbor-joining method.

Bacterial strains and growth conditions

Bacterial cells were grown in Todd Hewitt broth (THB) or in trypticase soy agar (TSA) supplemented with 5% sheep blood at 37°C.

Cloning, expression, and purification of recombinant proteins

Genes coding for the structural proteins of PI-2a were PCR amplified from GBS strain 515, expressed as His-tagged fusion proteins, and purified as already reported (2). PCR fragments encoding different forms of SrtC1 (SAL_1484) were cloned into pENTR/TEV/D-TOPO vector (Invitrogen, Carlsbad, CA, USA) and then subcloned into pET54 DEST vector (Novagen, San Diego, CA, USA) by Gateway LR reaction (Invitrogen) to generate His-tagged proteins. The recombinant mutants $SrtC1_{C219A}$, $SrtC1_{R228A}$, and $SrtC1_{H157A}$ were generated by the polymerase incomplete primer extension (PIPE) method (19). The mutants $SrtC1_{43–292}$ and $SrtC1_{43–254}$ were expressed as His-MBP, TEV cleavable, fusion proteins to increase the expression and solubility of the enzymes. The recombinant mutants $SrtC1_{Y86A}$ and $SrtC1_{\Delta LID}$ were generated by PIPE mutagenesis using as template the His-MBP-$SrtC1_{43–292}$ protein. Protein expression was performed in *Escherichia coli* BL21 (DE3) cells (Novagen). The cells were grown in Luria-Bertani medium, or in M9 minimal medium containing 1 mg/ml of $(^{15}NH_4)_2SO_4$ for the expression of ^{15}N labeled samples, at 37°C until $OD_{600} \sim 0.7$ and then induced with 1 mM isopropyl-β-D-thiogalactoside for 5 h at 25°C. The soluble proteins were extracted by sonication in 50 mM Tris-HCl (pH 7.5), 250 mM NaCl, 10 mM imidazole, lysozyme, and DNase and purified by a FF-Crude His-Trap HP nickel chelating column (Amersham Biosciences, Piscataway, NJ, USA). The recombinant SrtC1, eluted with 300 mM imidazole, was concentrated by ultrafiltration to 10 mg/ml, and the buffer was exchanged using a PD-10 desalting column (Amersham Biosciences) equilibrated with TEV cleavage buffer (50 mM Tris-HCl, pH 8; 1 mM DTT; and 0.5 mM EDTA). The His tag and the His-MBP tag were cleaved with AcTEV protease (Invitrogen) and then removed by a subtractive immobilized metal affinity chromatography purification step. The protein abundance in pure fractions was quantified with the BCA assay (Pierce, Rockford, IL, USA).

Antibodies

Antisera specific for the recombinant proteins were produced by immunizing CD1 mice with the purified proteins as previously reported (2).

Crystallization, data collection, structure solution

Crystals of SrtC1 (SAL_1484) were grown at 20°C by the vapor diffusion method. Sitting drops were formed by mixing equal volumes (0.25 μl) of 20 mg/ml of SAL_1484 in crystallization buffer (50 mM Tris, pH 8.0; 150 mM NaCl; and 0.5 mM TCEP), and of a well solution consisting of 100 mM Tris (pH 8.5), 200 mM NaOAc, and 30% PEG-4000. Crystals of SAL_1484 belong to space group $P2_1$, and the asymmetric unit contains one SAL_1484 monomer with a solvent content of 20% (Matthews coefficient 1.55 $Å^3$/Da). Diffraction data were collected at −173°C on beamline 5.0.3 of the Advanced Light Source (Lawrence Berkeley National Laboratory, Berkeley, CA, USA) and were processed by using HKL2000 (20) and the CCP4 suite of programs (21). The structure of SAL_1484 was solved by molecular replacement in Phaser (22), using as search model coordinates of Protein Data Bank (PDB) entry 2W1J (14), with which SAL_1484 shares 60% sequence identity. The final model was refined using Phenix (23) and Coot (24). Model analysis was performed using Procheck (25), and figures were generated with Pymol (26).

NMR spectroscopy analysis

For NMR data acquisition, the samples were buffer exchanged using a PD-10 desalting column (Amersham Biosciences) equilibrated with 50 mM phosphate buffer (pH 6.5) and finally concentrated by ultrafiltration. ^{1}H-^{15}N heteronuclear single quantum coherence (HSQC) spectra were recorded at 25°C on a Bruker Avance III spectrometer (Bruker Corp., Billerica, MA, USA) operating at 600.13-MHz proton Larmor frequency, equipped with a triple-resonance three-channel instrument (TCI) cryoprobe incorporating a *z*-axis gradient. Standard ^{1}H-^{15}N HSQC pulse sequence was used, with pulsed field gradients for suppression of the solvent signal and spectral artifacts. All the ^{1}H-^{15}N HSQC spectra on different protein samples were performed in the presence of 7% D_2O for NMR spectrometer frequency lock, in the same conditions, using a spectral width of 9515.385 Hz and 2048 complex points in the ^{1}H dimension, and a spectral width of 2432.718 Hz and 256 complex points in the ^{15}N dimension. Processing of all the spectra has been obtained with Topspin 2.1 (Bruker).

To check for the presence of bound metal ions deriving from the cell culture broth, EDTA was added in increasing amounts to the ^{15}N SrtC1 sample, up to a final concentration of 3 mM (largely in excess with respect to the protein) in 50 mM phosphate buffer with 1.5 mM DTT (pH 6.5). The protein sample was then buffer exchanged in 50 mM hepes (pH 6.5) using a PD-10 desalting column (Amersham Bioscience). Increasing amounts of $CaCl_2$ were added up to a protein:ion molar ratio of 1:10. ^{1}H-^{15}N HSQC spectra were registered at every addition step.

Construction of complementation vectors and site-specific mutagenesis

The GBS-knockout (KO) mutant strain for both sortase C genes, Δ(SrtC1+SrtC2), was generated as previously reported (11). For the generation of complementation vectors, DNA fragments corresponding to SrtC1 (SAL_1484), SrtC2 (SAL_1483), and both SrtC genes were PCR amplified from GBS 515 genome, and the products were cloned into the E. *coli*-streptococcal shuttle vector pAM401/gbs80P+T (previously described; refs. 11, 27), containing the promoter and terminator regions of the *gbs80* gene (TIGR annotation SAG_0645). Site-directed mutagenesis of pAM_SrtC1 and pAM_(SrtC1+SrtC2) was performed using the PIPE method (19). The method was improved using LA polymerase and digesting DNA template with DPNI enzyme to optimize the protocol for large plasmids, as pAM401 vector containing the SrtC1 gene. Mutations were confirmed by DNA sequencing. All complementation vectors were electroporated into the KO strain Δ(SrtC1+SrtC2). Complementation was confirmed by checking the sortase C expression by Western blotting. For all complementation experiments, the empty pAM401/gbs80P+T plasmid, introduced into wild-type strain 515 and mutant strains, was used as a negative control.

Fluorescence resonance energy transfer (FRET) assay

The FRET assay was used to monitor the *in vitro* activity of the recombinant SrtC1. We used fluorescently self-quenched peptides, tagged with EDANS as fluorophore and DABCYL as quencher, containing the LPXTG-motif of PI-2a BP subunit. When the peptide is cleaved by sortase, the fluorophore EDANS group is separated from the quencher DABCYL group, resulting in an enhanced fluorescence signal. The activity test was performed in 20 mM HEPES buffer (pH 7.5), 50 μM SrtC1 enzyme, and 100 μM fluorogenic peptide. Reaction was started by the addition of enzyme and was monitored by measuring the increase in fluorescence every 20 min (λ_{ex}=336 nm, λ_{em}=490 nm) at 25°C on an InfiniteM200 spectrophotometer microplate reader (Tecan, Männedorf, Switzerland). The synthetic fluorogenic peptide DABCYL-KKVTIPQTGGIGT-EDANS (BP peptide) was purchased from Thermo Scientific Biopolymers (Waltham, MA, USA) and was dissolved in 50% DMSO.

Kinetic measurements

Kinetic data were obtained by incubating various concentrations of BP peptide that ranged from 2 to 256 μM with a constant enzyme concentration of 25 μM. As control, the same peptide concentrations were incubated without the enzyme. All reactions were performed at 37°C in 20 mM HEPES (pH 7.5), 75 mM NaCl, and 1 mM DTT; reactions were initiated by the addition of enzyme and monitored by measuring the increase in fluorescence every 20 min for 780 min (λ_{ex}=336 nm, λ_{em}=546 nm) on an InfiniteM200 spectrophotometer microplate reader (Tecan). Assays were carried out in 96F black microplate for fluorescence reading (Nunc Thermo Fisher Scientific, Roskilde, Denmark).

Initial velocities (V) were determined from the progress curves and plotted against substrate concentration. The data were fitted to the Michaelis–Menten equation $V = V_{max}[S]/(K_m + [S])$ with a nonlinear regression analysis program. The best fits of the data produced V_{max} and K_m values, where V_{max} represents the maximum rate of peptide cleavage and K_m, the Michaelis constant, corresponding at the substrate concentration that produces exactly half of the maximum reaction rate, 0.5 V_{max}.

Western blotting analysis

Midexponential phase bacterial cells were resuspended in 50 mM Tris-HCl containing 400 U of mutanolysin (Sigma-Aldrich, St. Louis, MO, USA) and Complete protease inhibitors (Roche, Basel, Switzerland). The mixtures were then incubated at 37°C for 1 h and cells lysed by 3 cycles of freeze-thawing. Cellular debris were removed by centrifugation, and protein concentration was determined using BCA protein assay (Pierce). Subcellular fractionation of GBS was performed as previously reported (28). Briefly, bacteria were resuspended in an ice-cold protoplasting buffer containing 40% sucrose in 0.1 M K_3PO_4 (pH 6.2) and protease inhibitors. Cell walls were solubilized adding 400 U of mutanolysin for 30 min at 37°C. After centrifugation, the supernatant (cell wall fraction) was transferred to a fresh tube, and the cell pellet (protoplasts) were lysed in 100 mM NaCl, 100 mM Trizma-base (pH 7.5), and 10 mM $MgCl_2$ by 3 cycles of freeze-thawing. By ultracentrifugation at 436,000 g at 4°C for 30 min, the pellet (membrane fraction) was separated from the supernatant (cytoplasmic fraction) and solubilized using 2% SDS buffer.

Total protein extracts (20 μg) were resolved on 3–8 or 12% NuPAGE precast gels (Invitrogen) and transferred to nitrocellulose. Membranes were probed with mouse antiserum directed against structural pilus proteins (1:1000 dilution) or against SrtC1 enzyme (1:500 dilution), followed by a rabbit anti-mouse horseradish peroxidase-conjugated secondary antibody (Dako, Glostrup, Denmark). Bands were then visualized using an Opti-4CN substrate kit (Bio-Rad) or SuperSignal West Pico chemiluminescent substrate (Pierce).

RESULTS

Class C sortases in GBS

Comparative genome analysis of the available genomes of GBS enabled us to identify 32 genes predicted to express class C sortase enzymes. Sequence comparison by multiple alignment and phylogenetic analysis permitted the identification of 3 major clusters, corresponding to class C sortases of PI-1, PI-2a, and PI-2b, with amino acid identities ranging from 15 to 60% (**Fig. 1**). While both variants of PI-2 (PI-2a and PI-2b) contain 2 sortase genes (SrtC1 and SrtC2), PI-1 carries a third gene (SrtC3) predicted to code for a C sortase not directly involved in pilus polymerization (11, 29, 30). In the present study, the crystal structure of the sortase SrtC1 of PI-2a (SAL_1484) was solved at high resolution.

Overall folding of SAL_1484 and active site organization

The ectodomain of sortase SrtC1 of PI-2a (residues 43–254) was crystallized as a monomer in space group $P2_1$, and the structure was solved by molecular replacement (**Table 1**), using as the initial search model the coordinates of sortase C1 of *S. pneumoniae* (PDB 2W1J). The refined model of SrtC1 includes residues 47–252. The first 4 N-terminal and the final 2 C-terminal residues could not be modeled due to internal disorder. Two more regions could not be modeled due to their poor electron density maps: the first includes residues 95–96 of the mobile lid that covers the active site; the second is made by residues 240–249 at the C-terminal region (**Fig. 2*A***). The overall folding of GBS SrtC1 is highly similar to the folding of previously determined pilus-associated sortases (see structural comparison below). A β barrel made of 9 antiparallel β strands forms the core of the enzyme; a so-called roof made of 3 α helices positioned above the β barrel and a loop (known as the "mobile lid") that covers the active site. This last one is positioned on one inner side of the β-barrel core and is made of the catalytic triad His157-Cys219-Arg228. The lid of SrtC1 harbors 3 residues, Asp84, Pro85, and Tyr86 (Fig. 2), which make interactions with residues of the active site and surroundings. While Asp84 and Pro85 are highly conserved, an aromatic residue (Tyr86 in SAL_1484) generally occupies the third position (Fig. 2*B*). The carboxylate group of

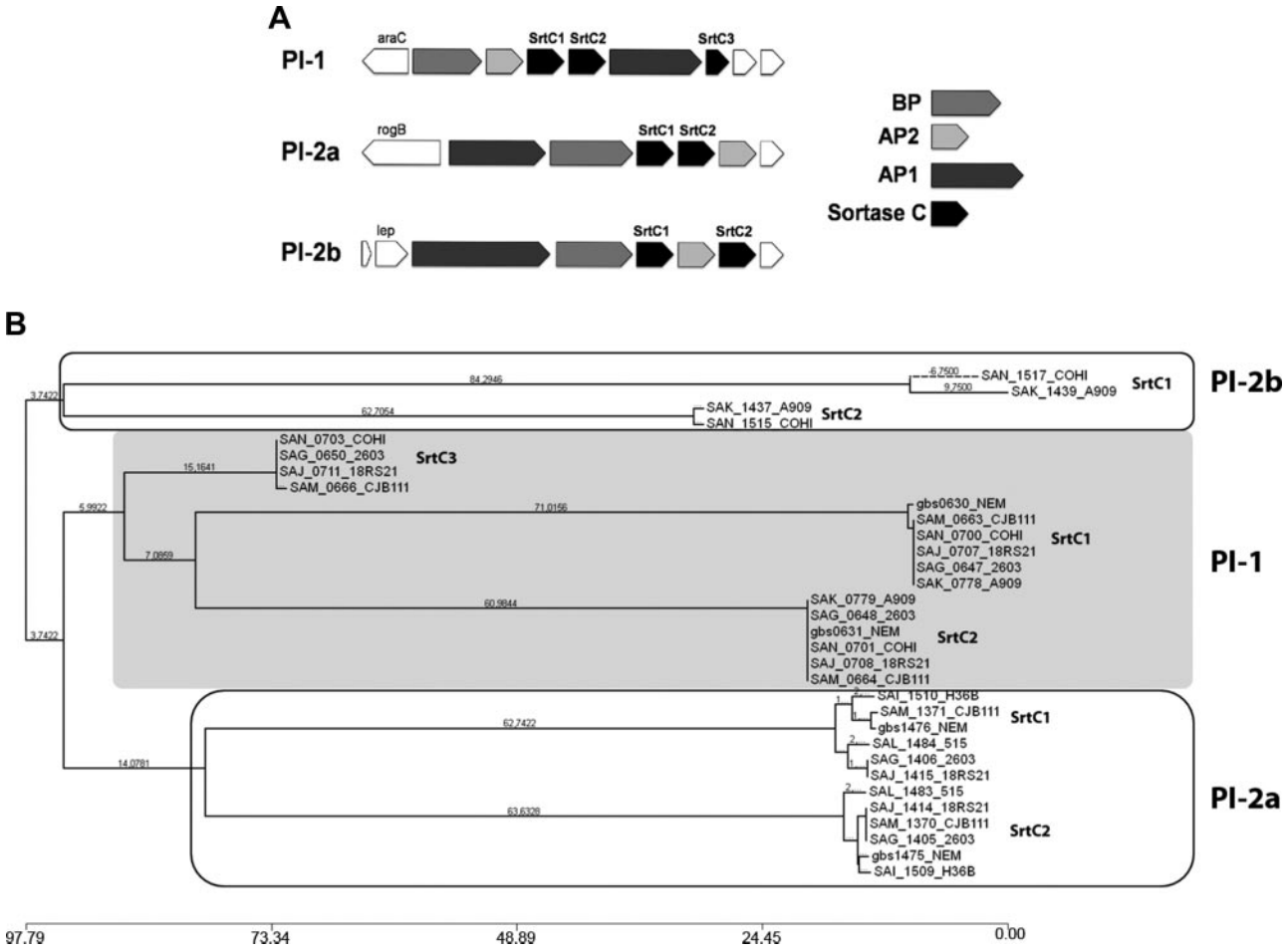

Figure 1. Class C sortases in PIs of GBS. *A*) Schematic representation of GBS PIs. *B*) Phylogenetic tree inferred from the alignment by the neighbor-joining distance-based method of C sortases from the available genomes of GBS. Single sortases are indicated by TIGR annotation. The 3 major clusters, highlighted in the boxes, include C sortases of each PI.

TABLE 1. *Data collection and refinement statistics*

Parameter	SAL_1484
Data collection	
Space group	$P2_1$
Cell dimensions	
a, *b*, *c* (Å)	45, 37.3, 51.2
α, β, γ (deg)	90, 96.7, 90
Resolution (Å)	50–1.3 (1.35–1.3)
R_{sym} or R_{merge} [a]	9.7 (41.2)
$I/\sigma I$	38.2 (2.3)
Completeness (%)	95.8 (71.1)
Redundancy	10.2 (4.4)
Refinement	
Resolution (Å)	1.3
Reflections	39,285
R_{work}/R_{free} [b]	15.4/18.1
Atoms	
Protein	2970
Water	175
B factor	
Protein	15.6
Water	16.6
RMSD	
Bond length (Å)	0.01
Bond angle (deg)	1.29
Ramachandran plot	
Favored	98.95
Allowed	1.05
Outliers	0

Values in parentheses refer to the highest resolution shell. [a] $R_{sym} = \Sigma_{hkl} \Sigma_i |I_i(hkl) - \langle I_i(hkl)\rangle| / \Sigma_{hkl} \Sigma_i I_i(hkl)$. [b] $R_{work} = \Sigma ||F_{obs}| - |F_{calc}|| / \Sigma |F_{obs}|$; R_{free} as for R_{work}, but for 5.0% of the total reflections chosen at random and omitted from refinement.

Asp84 forms a salt bridge with the side chain of the conserved catalytic residue Arg228 (Fig. 2*B*) and with a water molecule (W76). The ring of Tyr86 is positioned in a pocket lined by highly conserved hydrophobic residues (Leu131, Leu138, Val153, Leu217) on one side and by the catalytic residue His157 on the other side (Fig. 2*B*). The residue Pro85 points toward the same hydrophobic pocket (Fig. 2*B*). The aromatic benzene ring of Tyr86 is close enough to the catalytic Cys219 side chain to make an aromatic-sulfur interaction. As shown previously, this sulfur-aromatic interaction is conserved in other sortases (SrtB and SrtD), and this finding suggests that this serves as a general mechanism of anchoring the lid within the active site (ref. 31 and Fig. 2*B*). In addition, the hydroxyl group of Tyr86 makes H-bond interactions with the hydroxyl side chain of the highly conserved Thr155 and with the backbone amino group of the conserved Ala156 (Fig. 2*B*). The aromatic ring of Tyr86 is also positioned in a hydrophobic environment where it potentially can be involved in CH-π weak polar interactions. CH-π interactions have been shown previously to contribute to overall stability of proteins (32) However, closest CH-donors to Tyr86 are Leu131 and Pro85, with measured $d_{C\text{-}X}$ distances of 4.5 and 4.1 Å from the center of the π system, respectively (33). The side chains of lid residues 95 and 96 could not be modeled due to poor electron density, and residues 87–91 display *B* factors of 30–40 Å^2, which is considerably higher than the *B* factors for the overall structure (16 Å^2), suggesting a certain flexibility of this region, as previously observed in related structures from *S. pneumoniae* (14, 15, 34).

The active site of GBS SrtC1 is made of the highly conserved catalytic triad His157, Cys219, Arg228 (Fig. 2). His157 displays a single rotamer conformation and does not make interactions with surrounding residues. Cys219 adopts two alternative conformations, each modeled with 0.5 occupancies. The thiol group of one Cys219 conformer points toward His157, although it does not interact with the latter, being positioned 3.5 Å away from it. The second conformer points toward the aromatic ring of Tyr86, 2.9 Å distant. This sulfur-aromatic interaction has been postulated to strengthen the anchoring of the lid within the active site (15). The thiol group of the second conformer of Cys219 is within 4 Å from the Nε and NH1 of Arg228 (Fig. 2*B*). Furthermore, we also observed a water molecule (W22)

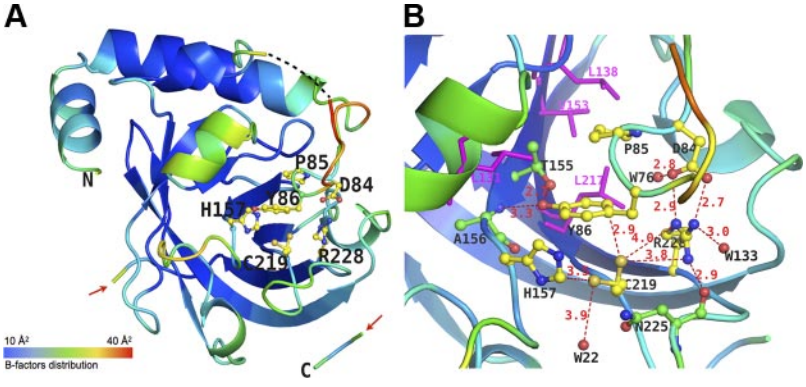

Figure 2. Overall folding of SAL_1484 and active site organization. *A*) Overall folding and *B* factors of SAL_1484. SAL_1484 is represented as a cartoon, colored according to *B*-factor distribution, from low (blue) to high (red). Residues forming the mobile lid and the active site are shown as balls and sticks and are labeled. N and C termini are labeled. Carbon, oxygen, and nitrogen atoms are depicted in yellow, red, and blue, respectively. Position of residues 92–93 of the mobile lid, missing from the model because of poor electron density, is indicated by black dashes. Red arrows indicate the gap in the C-terminal region, fragment of residues 240–249. *B*) Active site of SAL_1484. Residues forming the mobile lid (Asp84, Tyr86) and the active site (His157, Cys219, Arg228) are shown as balls and sticks, with carbon, oxygen, and nitrogen atoms in yellow, red, and blue, respectively. Conserved surrounding and interacting residues (Thr155, Ala156, Asn225) are shown as balls and sticks, with carbon, oxygen, and nitrogen atoms in green, red, and blue, respectively. Conserved hydrophobic residues are shown as magenta sticks and labeled in magenta. Distances between atoms are labeled and shown as red dashes. Water molecules are shown as red spheres. Background cartoon representation of SAL_1484 is colored according to *B* factors as in panel *A*.

located at a distance of 3.9 Å from Cys228; although this is not compatible with H-bonding distances, previous studies on sortases showed the formation of an H bond between this Cys and a conserved water molecule located nearby (15). Our observations support the same mechanism as in Neiers *et al.* (15); the presence of the dual conformation of Cys219 is likely a consequence of the binding of the substrate. On binding, disruption of the sulfur-aromatic interactions takes place, followed by the movement of the lid and thus the reorientation of the Cys side chain to form an H bond with a water molecule (15).

The side chain of Arg228 forms a salt bridge with the carboxylate group of Asp84 on the mobile lid. Also, Arg228 is within H-bonding distance from a water molecule (W133), and with the backbone carbonyl of the conserved residue Asn225 (Fig. 2*B*). This network of interactions between catalytic residues and those located on the lid (Asp84 and Try86) is postulated to regulate the movement of the lid and therefore the access of LPXTG substrates to the active site (34).

GBS SrtC1 is not involved in calcium binding

S. aureus housekeeping SrtA, which presents the same conserved catalytic triad of class C sortases (Supplemental Fig. S2), is reported to be a calcium-binding protein, and this binding is important for enzyme activity (35). The crystal structure of GBS SrtC1 reveals that the loop carrying the calcium-binding motif is not present, as in all crystal structures of class C sortase enzymes crystallized so far (Supplemental Fig. S1; refs. 14, 15). To confirm these data, we investigated the capability of GBS SrtC1 to bind calcium ions (or other metal cations) using NMR spectroscopy measurements. Monitoring the perturbations of ^{15}N and H_N chemical shifts on binding to a metal ion or to a ligand is commonly used to determine which residues are involved in interactions. To this end, ^{1}H-^{15}N HSQC spectra of ^{15}N-labeled SrtC1 were recorded at physiological pH in the absence and in the presence of a molar excess of $CaCl_2$. Prior to $CaCl_2$ addition, the protein was treated with EDTA to displace possibly bound calcium ions deriving from protein expression and purification steps. ^{1}H-^{15}N HSQC spectra were recorded before and after each addition of EDTA or calcium. No significant chemical shift changes of the amide resonances were observed, thus suggesting that SrtC1 does not bind metal ions in the broth and confirming that it does not bind calcium under these conditions (**Fig. 3**).

Structural comparison

A PDB search with the program DALI (36) returns 45 hits with a score of $Z > 2$. We analyzed by structural comparisons those entries with a score of $Z > 10$. The closest homologue of SAL_1484 is the transpeptidase sortase C1 (or B) of *S. pneumoniae* (PDB 2W1J), with root mean square deviation (RMSD) of 1.3 Å for 191 equivalent Cα atoms and 63% sequence identity (DALI; Z=33.6). Other homologues of SAL_1484 include the *S. pneumoniae* sortase C2 (or C; PDB 3G69, with sequence identity/RMSD of 50%/1.7 Å); the *S. pneumoniae* sortase C-3 (or D; PDB 2W1K, sequence identity/RMSD 28%/2.2 Å); sortase A of *Streptococcus pyogenes* (PDB 3FN7, sequence identity/RMSD, 26%/3.1 Å), sortase A of *S. aureus* (PDB 1IJA, sequence identity/RMSD, 25%/2.9 Å), the sortase B of *S. aureus* (PDB 1QWZ, sequence identity/RMSD 19%/3.5 Å), and sortase B of *Bacillus anthracis* (PDB 2OQZ, sequence identity/RMSD 18%/3.0 Å).

The central β-barrel core is highly conserved among all sortases analyzed (pilus-associated and housekeeping sortases as shown in Supplemental Fig. S2, top and bottom, respectively). The mobile lid and the 3 α

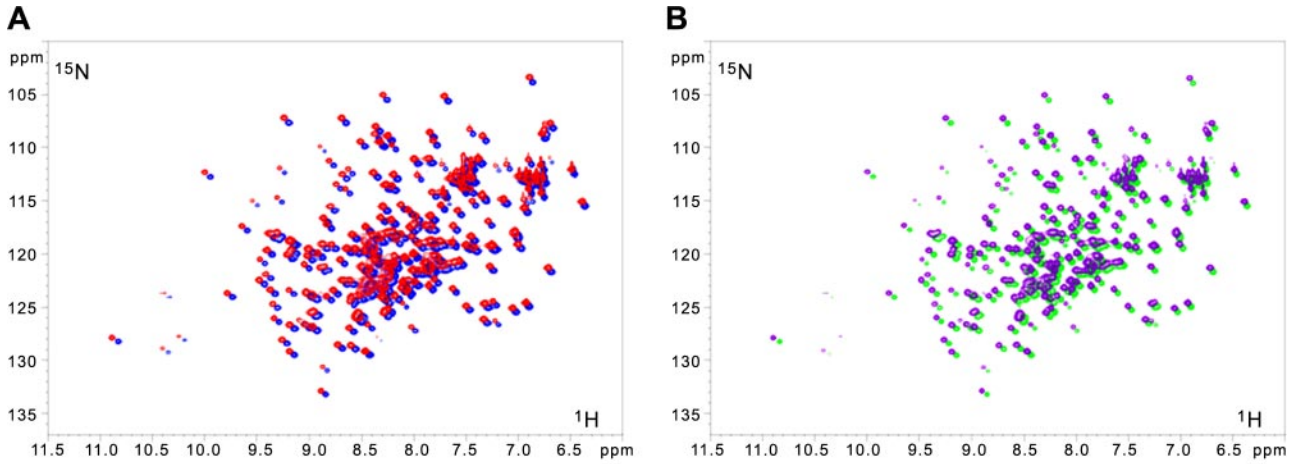

Figure 3. NMR spectroscopy assessment of metal ion binding by SrtC1. *A*) ^{1}H-^{15}N HSQC spectra recorded on ^{15}N-SrtC1 in 50 mM phosphate buffer and 1.5 mM DTT, pH 6.5 (red), with addition of 3 mM EDTA (blue). *B*) ^{1}H-^{15}N HSQC spectra recorded on ^{15}N-SrtC1 in 50 mM hepes, pH 6.5 (violet), with addition of $CaCl_2$ at a protein:calcium molar ratio of 1:10 (green). For reasons of clarity, the overlaid spectra (blue and green) in each panel are shown with an offset of 0.8 and 0.4 ppm in the ^{1}H and ^{15}N dimensions, respectively.

helices that form the roof are conserved only among pilus-associated sortases (14).

The multiple sequence alignment performed with all the available GBS sortase C enzyme sequences revealed that the lid is not ubiquitously present (data not shown). The sequences of SAN_1515 and SAK_1437, corresponding to SrtC2 of PI-2b in 2 sequenced GBS strains, form a cluster far away from the others, sharing just a short central portion of the sequence and not the conserved N and C termini. These enzymes lack the predicted C-terminal TM helix, while they retain the one at the N terminus. The lid is unlikely to be present in this sortase C class, since the main hydrophobic core is linked to the N-terminal TM helix by a connecting sequence missing more than 30 residues compared to the other sortase C sequences. To investigate its structural and functional roles, we generated a comparative homology model of sortase SAK_1437, a particular class C sortase predicted to lack a lid. The superimposition between the crystal structure of SAL_1484 and the model of SAK_1437 revealed that except for the missing lid region, the overall folding is highly conserved (RMSD=1.3 Å; **Fig. 4**).

PIPE method applied to large plasmids allowed the generation of complementation mutants of selected amino acids in sortase C genes

To functionally characterize the role of selected conserved amino acid motives and residues in the SrtC1 sequence, we generated several single-substitution mutations as well as deletions using the PIPE method (19) on the large vector pAM401/gbs80 P+T previously generated (11) and used in complementation studies of GBS-KO mutant strains (11). As template for the introduction of specific mutations, we used the complementation vector pAM_(SrtC1+SrtC2) carrying both sortase genes of PI-2a under the control of the GBS80 promoter, which had previously been shown to function well in GBS and overexpress different proteins (11). Replacement of selected amino acid residues was done individually with synthetic oligonucleotide primers. The complementation vectors carrying the specific mutations were then used in restoring the activity of the enzymes by transforming the double isogenic KO mutant strain 515Δ(SrtC1+SrtC2) lacking both the sortase C genes. After complementation of KO strains, the effect of each mutation or deletion was analyzed by Western blotting analysis, checking the polymerization of the BP and the incorporation into pili of the ancillary proteins. To validate the use of complementation studies for evaluating the sortase C activity, we first generated complementation vectors pAM_SrtC1, pAM_SrtC2, and pAM_SrtC1+SrtC2 carrying the wild-type SrtC1, SrtC2, or both sortase C genes, respectively, and used these plasmids to transform the pilus polymerization-defective GBS-KO mutant strain lacking both sortases, 515Δ(SrtC1+SrtC2) (11). As expected, complementation of this mutant strain with a single gene (SrtC1 or SrtC2) or both wild-type sortase C genes restored pilus polymerization and also confirmed the specificity in the recognition and/or incorporation into pili of the accessory subunits AP1 and AP2 (Supplemental Fig. S3).

Catalytic triad C219, H157, and R228 of GBS SrtC-1 is absolutely required for pilus polymerization

To confirm the key role of the catalytic triad C219, H157, and R228 for GBS SrtC1 activity, each residue was replaced individually by an alanine into the complementation plasmid pAM_SrtC1. Complementation was performed by transforming the double mutant 515Δ(SrtC1+SrtC2) with recombinant plasmids expressing mutated sortases ($SrtC1_{C219A}$, $SrtC1_{R228A}$, and $SrtC1_{H157A}$). Western blotting analysis performed with total protein extracts from complemented strains confirmed that polymerization of pilus proteins was completely abolished (**Fig. 5*A***, top panel). The same result was obtained by substitution of the C222 with alanine in

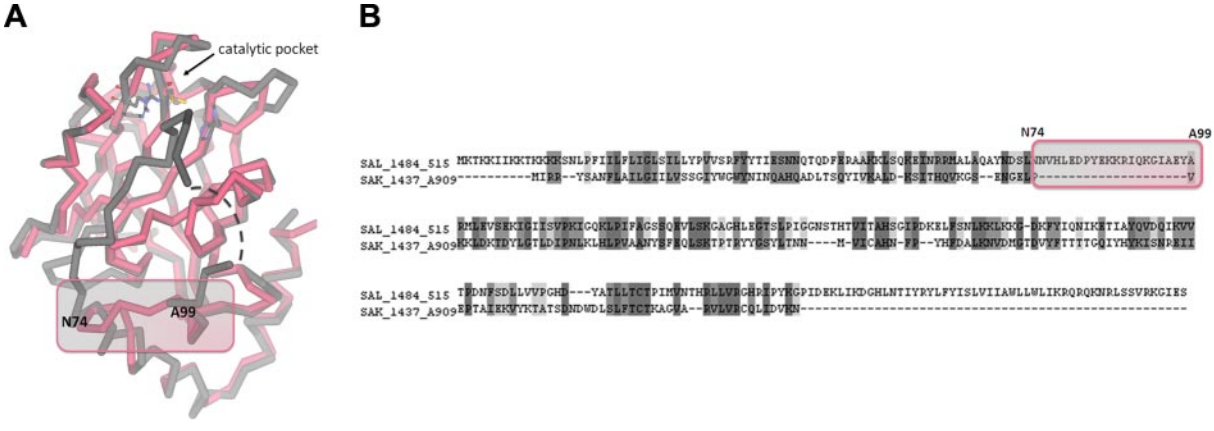

Figure 4. C sortases of PI-2b do not contain the lid region. *A*) Structural comparison of the crystal structure of GBS SrtC1 of PI-2a, SAL_1484, (dark gray) and the modeled structure of SrtC2 of PI-2b, SAK_1437 (purple). Catalytic pocket of SAL_1484 is indicated. Positions N74 and A99, at which SAL_1484 differs from SAK_1473, are highlighted in box. *B*) Sequence alignment of SAL_1484 and SAK_1473. Sequence corresponding to the lid region of SAL_1484 is highlighted in box.

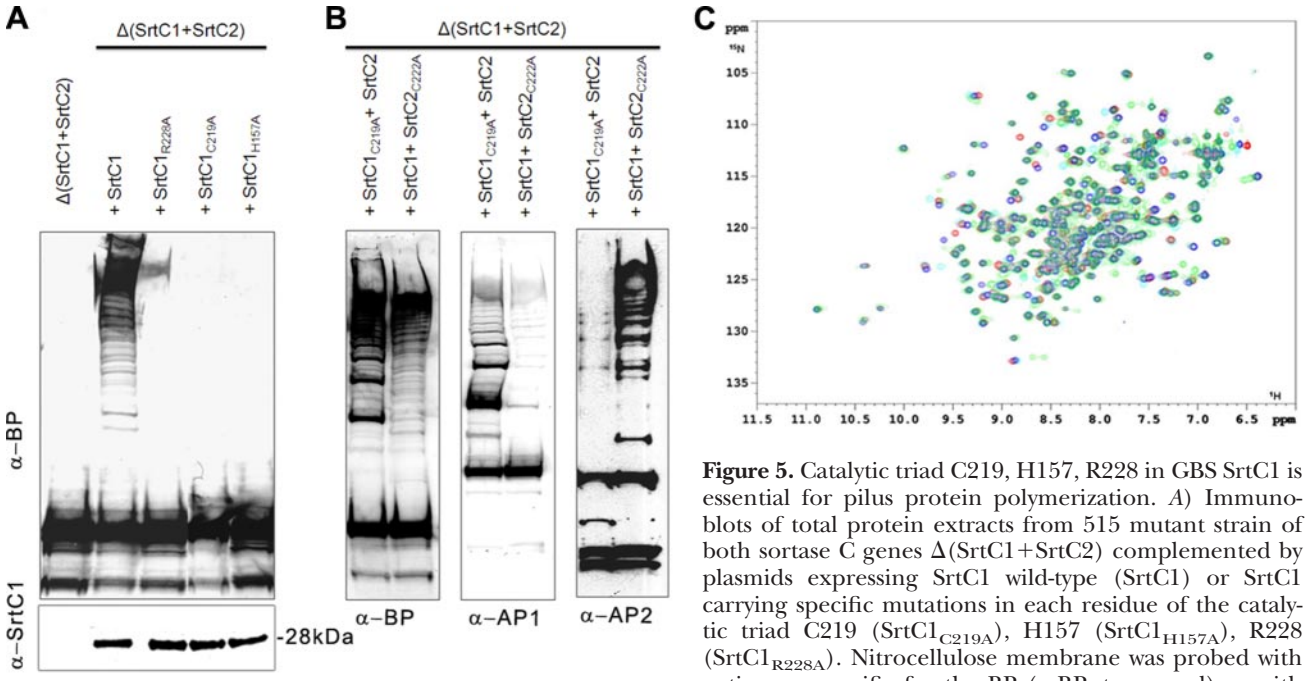

Figure 5. Catalytic triad C219, H157, R228 in GBS SrtC1 is essential for pilus protein polymerization. *A*) Immunoblots of total protein extracts from 515 mutant strain of both sortase C genes Δ(SrtC1+SrtC2) complemented by plasmids expressing SrtC1 wild-type (SrtC1) or SrtC1 carrying specific mutations in each residue of the catalytic triad C219 ($SrtC1_{C219A}$), H157 ($SrtC1_{H157A}$), R228 ($SrtC1_{R228A}$). Nitrocellulose membrane was probed with antiserum specific for the BP (α-BP, top panel) or with antiserum raised against sortase C1 (α-SrtC1, bottom panel). *B*) Immunoblots of total protein extracts from mutant strain Δ(SrtC1+SrtC2) complemented by plasmids expressing both sortases C (SrtC1 and SrtC2) with catalytic Cys residue mutated one by one ($SrtC1_{C219A}$+SrtC2) and (SrtC1+$SrtC2_{C222A}$). Nitrocellulose membranes were probed with antisera specific for the BP (α-BP) and the ancillary proteins (α-AP1 and α-AP2). *C*) Superimposition of NMR ^{1}H-^{15}N HSQC spectra of SrtC1 wild-type and its mutants. Red, SrtC1 wild-type; blue, $SrtC1_{C219A}$; cyan, $SrtC1_{H157A}$; light green, $SrtC1_{R228A}$. All samples are in 50 mM phosphate buffer, pH 6.5.

the SrtC2 gene (data not shown). Antibodies specific for SrtC1 revealed that all the mutant strains expressed similar levels of the different forms of SrtC1, indicating that none of the introduced mutations had seriously affected the expression or the stability of the proteins (Fig. 5*A*, bottom panel). Moreover, when the catalytic C219 of SrtC1 and C222 of SrtC2 were mutated alternately into alanine in the plasmid carrying both sortase genes, the BP was still polymerized, as at least one SrtC was still active (Fig. 5*B*). On the other hand, immunoblotting analysis using antibodies raised against the ancillary proteins AP1 and AP2 revealed AP2-containing HMW polymeric forms mostly in protein extracts from strains in which the SrtC1 contained the catalytic cysteine, while AP1 was prevalently polymerized when SrtC2 was active (Fig. 5*B*). These data represent a further confirmation of the specificity of the SrtC enzymes for the incorporation of the ancillary proteins into pili and their redundancy for the BP polymerization.

To investigate whether the mutations in the catalytic cleft affect the general folding of the mutated proteins, the mutants $SrtC1_{C219A}$, $SrtC1_{R228A}$, and $SrtC1_{H157A}$ were produced as recombinant ^{15}N-labeled proteins and analyzed by NMR spectroscopy. The ^{1}H-^{15}N HSQC spectrum is a valuable tool to evaluate protein folding, as the secondary and tertiary structures determine unique chemical environments of amide groups, which are reflected by significant signal dispersion in both the nitrogen and proton dimensions. The analysis of the HSQC spectra of the mutants of SrtC1 showed that the large majority of amide signals overlapped with those of the wild-type protein (Fig. 5*C*). Chemical shift perturbations observed for a small number of peaks in all 3 samples can be attributed to local changes in chemical properties introduced around the respective mutation sites. Overall, it can be concluded that the mutated residues do not cause structural destabilization of the SrtC1 enzyme, as the native folding is preserved.

Finally, to investigate whether additional residues could be involved in the enzymatic activity of GBS SrtC enzymes, we tested the role of the highly conserved amino acids Asn225 and the Pro221 located close to the catalytic cysteine. We found that neither P221A nor N225A substitutions prevented the pili polymerization, as all the mutated strains could efficiently polymerize the BP and incorporate the ancillary proteins into HMW forms as well as the wild-type strain (data not shown).

In summary, these data confirm that, as for the other members of the sortase family (14, 15, 34), the GBS sortase SrtC1 requires a catalytic triad composed of C219, H157, and R228 for pilin polymerization.

Lid region is not essential for pilus polymerization

Structural studies of the C sortases of *S. pneumoniae* have shown that the accessibility of the catalytic site is controlled by the presence of a flexible lid (14, 15, 34). The lid of GBS SrtC1 corresponds to residues 81–96 and harbors 3 conserved residues (Asp84, Pro85, and

Tyr86), which interact with residues of the active site and surroundings residues. The relative organization of the Cys219 residue in the active site and the 4 conserved polar amino acids (His157 and Arg228 of the catalytic triad and Asp84 and Tyr86 of the lid) is very similar to that of pneumococcal SrtC1 (14, 15). To investigate the function of the lid region for the sortase C1 activity in polymerization of pilus proteins, we generated complementation plasmid mutants carrying the substitutions D84A and Y86A singularly, or the deletion of the entire lid loop spanning from aa 81 to 96. As for the mutants of the catalytic triad and the wild type, the complemented strains resulted in an overexpression of the SrtC1 enzymes. None of the introduced mutations in the lid abrogated pilus protein polymerization (32, 33), as revealed by immunoblotting analysis of protein extracts from complemented strains. In effect, both the backbone subunit (**Fig. 6**) and the ancillary proteins (Fig. 6*B*, *C*) could assemble in covalently linked high-molecular-weight polymers.

To investigate the role of the lid region in pilus biology, we tested by FRET assay the *in vitro* enzymatic activity of the purified recombinant sortases $SrtC1_{WT}$, $SrtC1_{Y86A}$, the mutant of the lid residue Tyr86, and $SrtC1_{\Delta LID}$, the enzyme containing the deletion of the entire lid region using fluorogenic peptides mimicking the LPXTG motif of the pilus 2a BP (BP peptide). FRET analysis is commonly used to follow transformation of substrates by enzymes, such as sortases (37). We performed a kinetic analysis of the peptide cleavage reaction at various concentrations of BP peptide when the enzyme concentration was fixed at 25 μM (**Fig. 7*A***). An increase of the fluorescence signal (normalized against the fluorescence values of the peptide alone) was observed for all 3 enzymes tested, indicating that the enzymes containing the mutation of the Tyr86 or the deletion of the entire lid region were still active, according to the data obtained by *in vivo* mutagenesis. At low substrate concentrations (<10% reaction) the rate of increase in the fluorescence signal *vs.* substrate concentration fits the Michaelis-Menten equation (Fig. 7*B*). Kinetic characterization of enzymes (546 nm) with substrate (2–256 μM) yielded an apparent K_m of 13.8 μM and an apparent V_{max} of 10.0 relative fluorescence units (RFU)/min for $SrtC1_{WT}$, apparent K_m of 29.4 μM and V_{max} of 19.9 RFU/min for $SrtC1_{Y86A}$, and apparent K_m of 63.9 μM and V_{max} of 30.5 RFU/min for $SrtC1_{\Delta LID}$. The apparent V_{max} reached by the $SrtC1_{\Delta LID}$ is 3-fold higher than that of wild-type enzyme, and the apparent V_{max} of $SrtC1_{Y86A}$ is ~2-fold higher than that of $SrtC1_{WT}$. Within the range of substrate concentration tested, the estimated apparent K_m and the V_{max} values indicate that the mutants can still recognize and cleave the peptide at least as well as the wild-type protein.

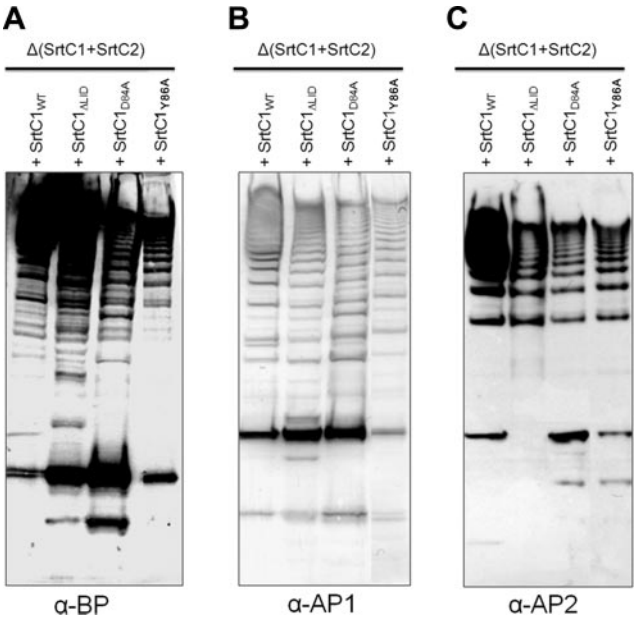

Figure 6. Lid region is not essential for pilus protein polymerization. Immunoblots of total protein extracts from 515 mutant strain of both sortase C genes Δ(SrtC1+SrtC2) complemented by plasmids expressing SrtC1 wild-type ($SrtC1_{WT}$) or SrtC1 carrying the mutation D84A ($SrtC1_{D84A}$) or Y86A ($SrtC1_{Y86A}$) or the deletion of the entire lid region ($SrtC1_{\Delta lid}$). Nitrocellulose membranes were probed with antisera specific for the BP (*A*) and the ancillary proteins, AP1 (*B*) and AP2 (*C*).

Predicted C- and N-terminal TM domains of SrtC1 are required for efficient pilus polymerization

To investigate the role in pilus polymerization of the SrtC1 N-terminal TM region, predicted to be part of the leader sequence, and the C-terminal TM positively charged tail, we generated SrtC1 mutants by deleting either only the C-terminal positive tail or the entire C- and N-terminal TM regions, singly or together (**Fig. 8*A***). The deletion of only the C-terminal positively charged tail did not affect either BP polymerization (Fig. 8*B*) or ancillary protein incorporation (data not shown). However, polymer formation was abrogated completely when the entire N- and C-terminal TM domains were deleted, both singly and together (Fig. 8*B*). Same results were also observed in SrtC2 mutants lacking the C- and N-terminal TM regions (data not shown), confirming the key role of these regions for the activity of the class C sortase enzymes. To better explore the role of the C-terminal TM domain in sortase activity, we generated a chimera by inserting into the SrtC1 gene the C-terminal TM and positively charged tail from the corresponding region belonging to the BP of pilus 2a (BP-2a; Fig. 8*A*). Interestingly, the activity of this chimeric enzyme was not efficient in restoring the backbone polymerization, confirming the importance of the original sequence for enzyme function (Fig. 8*B*).

To verify the expression and the correct localization of all the mutated forms of SrtC1 expressed in the complemented strains [double mutant Δ(SrtC1+SrtC2) complemented with SrtC1 wild-type, SrtC1 lacking the N-terminal, the C-terminal, or both the TM regions, and the SrtC1 chimera containing the C-terminal TM region of the BP], we performed a cell fractionation of GBS cul-

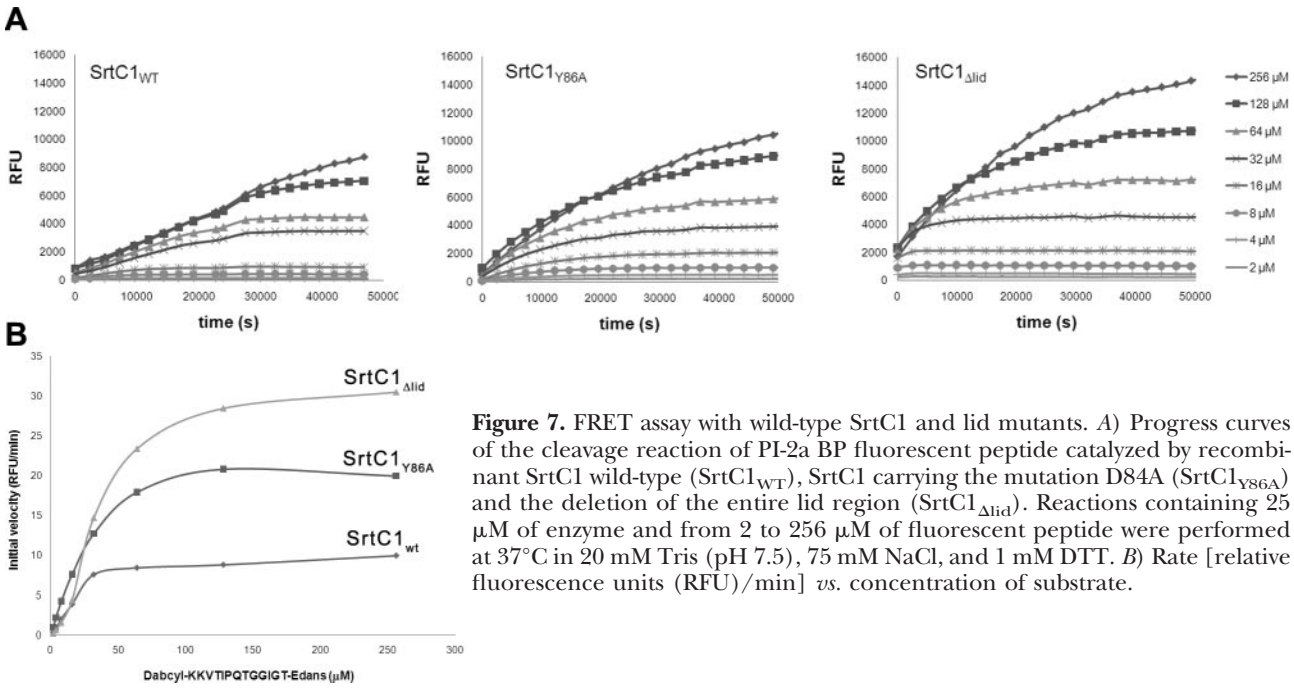

Figure 7. FRET assay with wild-type SrtC1 and lid mutants. *A*) Progress curves of the cleavage reaction of PI-2a BP fluorescent peptide catalyzed by recombinant SrtC1 wild-type ($SrtC1_{WT}$), SrtC1 carrying the mutation D84A ($SrtC1_{Y86A}$) and the deletion of the entire lid region ($SrtC1_{\Delta lid}$). Reactions containing 25 μM of enzyme and from 2 to 256 μM of fluorescent peptide were performed at 37°C in 20 mM Tris (pH 7.5), 75 mM NaCl, and 1 mM DTT. *B*) Rate [relative fluorescence units (RFU)/min] *vs.* concentration of substrate.

tures. Equal amounts of protein extracts from each of 3 different subcellular fractions obtained (the cell wall on solubilization by enzymatic hydrolysis and the soluble cytoplasmic and membrane fractions) were analyzed by immunoblotting using anti-SrtC1 antibodies. All of the 28-kDa SrtC1 proteins were detected at a similar level in the membrane fraction (Fig. 8*C*), indicating that none of the mutations introduced had affected the expression of the mutated SrtC1 genes or the SrtC1 localization into the membrane. Only when both the predicted TM regions were deleted was most of the enzyme found in the cytoplasmic fraction, suggesting that at least one of the two hydrophobic regions is necessary for sortase localization in the cellular membranes (Fig. 8*C*).

We further confirmed the functional role of the C-terminal TM region in SrtC enzymes by *in vitro* FRET assay using recombinant sortase proteins. We cloned, expressed, and purified the GBS SrtC1 enzyme of PI-2a

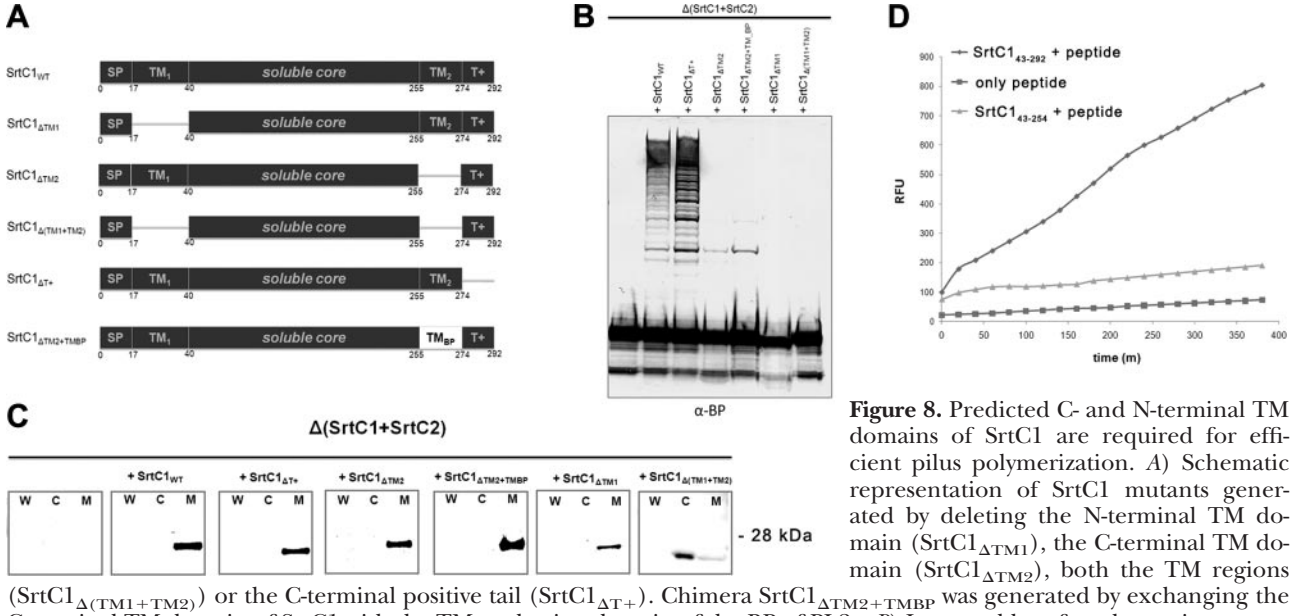

Figure 8. Predicted C- and N-terminal TM domains of SrtC1 are required for efficient pilus polymerization. *A*) Schematic representation of SrtC1 mutants generated by deleting the N-terminal TM domain ($SrtC1_{\Delta TM1}$), the C-terminal TM domain ($SrtC1_{\Delta TM2}$), both the TM regions ($SrtC1_{\Delta(TM1+TM2)}$) or the C-terminal positive tail ($SrtC1_{\Delta T+}$). Chimera $SrtC1_{\Delta TM2+TMBP}$ was generated by exchanging the C-terminal TM domain of SrtC1 with the TM anchoring domain of the BP of PI-2a. *B*) Immunoblot of total protein extracts from TM mutants of SrtC1 probed with antiserum specific for the BP. *C*) Immunoblot of the subcellular fractions, the cell wall (W), cytoplasm (C), or membrane (M) of the TM mutants of SrtC1 probed with mouse serum anti-SrtC1. *D*) FRET assay for evaluating the *in vitro* enzymatic activity of recombinant sortase proteins, $SrtC1_{43–254}$, lacking the leader sequence, the N- and C-terminal hydrophobic regions, and $SrtC1_{43–292}$, preserving the C-terminal TM region and lacking only the leader sequence and the N-terminal region. $SrtC1_{43–292}$ (50 μM) can catalyze the hydrolysis of 100 μM of fluorogenic peptide, which is not hydrolyzed by $SrtC1_{43–254}$.

as recombinant proteins in two forms, one $SrtC1_{43–254}$, lacking the leader sequence and the N- and C-terminal hydrophobic regions, and the other $SrtC1_{43–292}$, preserving the C-terminal TM region and lacking only the leader sequence and the N-terminal region. The activity of the recombinant enzymes was tested using fluorescent peptides mimicking the natural BP substrates. The same experiment was performed by using recombinant SrtC2 of GBS PI-2a and recombinant SrtC1 and SrtC2 of GBS PI-1 (data not shown). For all the purified enzymes, we observed that an increase of fluorescence was present only when the enzymes contained the C-terminal TM region, confirming the essential role of this domain for sortase C activity (Fig. 8*D*).

DISCUSSION

Several species of gram-positive pathogens encode sortase enzymes, specific membrane-anchored transpeptidases that are involved in anchoring virulence factors to the cell wall envelope (9). These enzymes are grouped in more than one class on the basis of sequence homology and distinct function (9, 38, 39). GBS encodes for a class A housekeeping sortase, responsible for the cell wall anchoring of surface proteins and for pilus-related class C sortases playing a key role in pilus biogenesis (11). In the present study, we applied a multidisciplinary approach including *in silico* analysis, structural and biochemical studies, and *in vivo* mutagenesis to characterize the pilus-associated sortase C1 of GBS PI-2a, allowing us to delineate the minimal region required for catalysis, to define nonessential (and essential) amino acids, and to corroborate structure-based predictions. The SrtC1 enzyme was expressed in a recombinant form lacking both N- and C-terminal TM regions, and the purified protein was found to be folded correctly and monomeric in solution by NMR analysis (data not shown). Previously reported NMR data on SrtA of *S. aureus* describe large chemical shift changes in the amide nitrogen and proton atoms of residues localized in the β3–β4 and β6–β7 loops on calcium ion addition, leading to the prediction that residues E105, E108, and E112 within the β3–β4 loop and E171 from β6–β7 loop form a structurally ordered calcium-binding site (40). The absence of significant NMR chemical shift change on addition of EDTA or $CaCl_2$ to GBS SrtC1 indicates that, while calcium binding is required for the activity of the housekeeping SrtA in *S. aureus* (35), GBS SrtC1 does not bind any calcium ion.

The high-resolution crystal structure of GBS SrtC1 revealed that the overall folding of the enzyme is highly similar to the folding of previously determined 3-D structures of pilus-associated sortases (14, 15). The active site of SrtC1 is positioned on one side of the β-barrel core and is made of the catalytic triad His157-Cys219-Arg228, absolutely required for the enzyme activity. Through site-directed mutagenesis and *in vivo* complementation studies, we have demonstrated that each residue in the catalytic triad is essential for pilus polymerization; these data confirm the relationship between GBS C sortases and other members of sortase family. An evolutionary conservation analysis of representative members of the family of sortases was performed by Consurf (41). The first 50 hits obtained by BLAST search with the primary sequence of SAL_1484 were utilized to prepare a multiple sequence alignment that was then given as input to Consurf. The coordinates of GBS SrtC1 were also given as input to Consurf for mapping residue conservation scores into the 3-D structure. This analysis revealed the central β core harboring the active site as the largest and most highly conserved region among all sortases analyzed, including also the housekeeping sortases, as compared with the rest of the protein, and the region that surrounds the β core as moderately conserved (**Fig. 9**). In particular, the cysteine residue, which represents the nucleophile where the LPXTG motif is covalently linked, is universally conserved in the sortase family (9, 16, 17). In contrast, residues of the lid are highly variable.

To understand whether the mutations C219A, H157A, and R228A in the catalytic triad of SrtC1 of *S. agalactiae* have an effect on enzyme folding, the ^{1}H-^{15}N HSQC spectra of these mutants were compared with the ^{1}H-^{15}N HSQC spectrum of the wild-type protein. The good spread and the partial overlap of the reso-

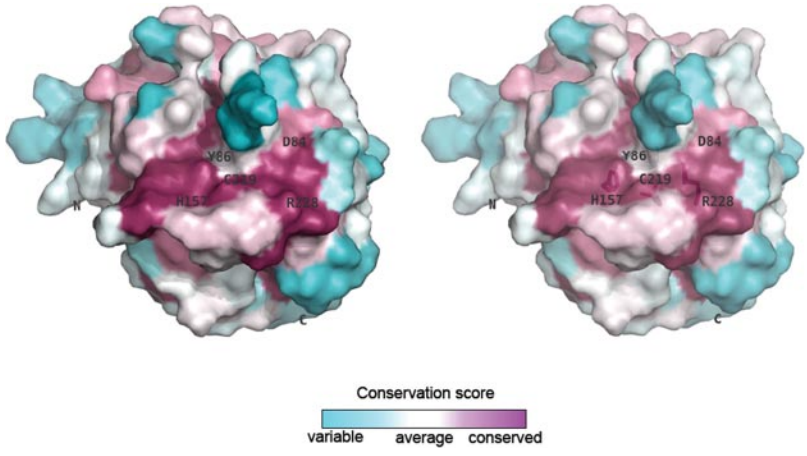

Figure 9. Conservation analysis of sortases by Consurf (41). SAL_1484 is represented as surface and colored according to the conservation score obtained from Consurf (see scale legend). Analysis includes the first 50 homologous hits obtained from BLAST search after submitting the full-length sequence of SAL_1484 (Supplemental Fig. S2). Active site and mobile lid residues are labeled and shown through transparent surface as sticks (right panel).

nances suggest that the mutations of residues of the catalytic triad do not induce structural destabilization of the SrtC1 enzyme and the native folding is preserved. From our data, it is evident that individual replacements of the 3 conserved residues C219, H157, and R228 have a direct effect on the enzymatic activity of SrtC1.

Recently, the function of the lid region has been investigated in the pilus fiber-formation activity of SrtC-1 from *S. pneumoniae*. From the analysis of the crystal structure of pneumococcal C sortases, Neiers *et al.* (15) suggest that the lid is a flexible region that could have a role for controlling the accessibility of the catalytic site and the enzyme stability. It has also been suggested that the presence of a flexible lid seems to be a specific feature of all pilus-related sortases (14, 15). The crystal structure of GBS SrtC1 shows that catalytic residues are not accessible to pilus substrates (Fig. 2), as they are locked by the lid. Moreover, our results demonstrate that the mutations of key residues Asp84 and Tyr86 in the lid region or the deletion of the entire lid region have no effect on pilus protein polymerization, although it looks like the amount of unprocessed BP is increased when the lid is mutated (Fig. 6*A*). To better investigate the role of this region in catalysis, we performed *in vitro* measurements of the kinetic properties of recombinant $SrtC1_{Y86A}$ and $SrtC1_{\Delta LID}$ in comparison with the $SrtC1_{WT}$. We found that, accordingly to the *in vivo* data, the lid mutants can efficiently cleave the substrate peptide, and the rate of peptide cleavage by lid mutant variants was even higher than that obtained with the wild-type enzyme. These results fit with the role of the lid suggested by the crystal structure, in which the lid covers the active site and sterically blocks the access of substrate. Our structural and biochemical data suggest that the lid maintains the enzyme in an inactive closed conformation and that, for the enzyme activation, the lid needs to move. We can therefore speculate that the deletion of the lid region does not abrogate pilus protein polymerization because its role is not catalytic; rather, it is a catalytic-cleft-blocking loop, and only its movement can activate the enzyme *in vivo*. The main questions remain to understand how this movement can be regulated by the interaction with the pilus proteins and to identify which are the residues involved in stabilizing the active open-lid conformation of the enzyme.

By multiple sequence alignment of all GBS sortase C enzymes and structural homology modeling, we also found that, in contrast with highly similar SrtC enzymes of PI-1 and PI-2a that also contain the lid region, the pilus-associated sortases of PI-2b are shorter. In addition, even if the catalytic triad is conserved, SrtC1 does not contain the conserved motif DPY(F/W) in the lid, and SrtC2 completely lacks the lid region (Fig. 4). PI-2b in GBS has a similar genetic organization to group A *Streptococcus* (GAS) FCT-3 pilus, and like GAS, it contains the LepA gene required in GAS for pilus polymerization (42). Further investigations will be needed for a better understanding of PI-2b class C sortases in pilus biogenesis.

Another interesting finding of this work is that the predicted C- and N-terminal TM domains of GBS SrtC1 are absolutely required for sortase biological function. Data obtained from the available crystal structures of C sortases show that these sortases can adopt a stable catalytically active conformation even in absence of the predicted C-terminal TM domain (14, 15, 34). However, the importance of TM domains for the enzyme activity has been recently reported for the pilus-associated sortase of *Corynebacterium diphtheriae*. Ton-That and co-workers (43) showed that the predicted C-terminal TM domain of pilus-associated sortase SrtA is essential for efficient pilus polymerization in *C. diphtheriae*. In addition, the evidence that the substitution in GBS SrtC1 of the C-terminal TM region with the corresponding hydrophobic helix of the backbone subunit of pilus type 2a could not restore enzyme activity strengthens the view that this region could play a key role in enzyme function. Finally, also in an *in vitro* FRET assay using fluorescent peptides mimicking the natural LPXTG substrates, the activity of SrtC enzymes was detected only when the enzyme contains the C-terminal TM region. Taken together, our data suggest that the N-terminal hydrophobic helix could have a role in protein anchoring to the membrane, while the C-terminal TM region could be also involved in enzyme activity. Although we could not so far obtain crystals of the recombinant enzyme containing the C-terminal TM region, elucidating the role that this might play on catalysis will be the result of future studies.

In summary, the multidisciplinary approach used in this work, including the PIPE mutagenesis method, implemented for a rapid mutagenesis of large plasmids used for gram-positive bacteria complementation studies and our findings could be extended to all sortase C enzyme classes based on the phylogenetic tree and structural similarities. FJ

The authors are grateful to Glen Spraggon (Genomics Institute of the Novartis Research Foundation, San Diego, CA, USA) and to Matthew Bottomley (Novartis Vaccines, Siena, Italy) for valuable discussions and critical review of the manuscript. The authors thank Prof. Tom Alber (University of California, Berkeley, CA, USA) for fruitful discussion of the sortase enzyme structures. The authors thank Roberto Rosini (Novartis Vaccines) for providing the GBS KO strain 515Δ(SrtC1+SrtC2). R.C. is the recipient of a Novartis fellowship from the Ph.D. program in Cellular, Molecular and Industrial Biology of the University of Bologna (Bologna, Italy).

REFERENCES

1. Johri, A. K., Paoletti, L. C., Glaser, P., Dua, M., Sharma, P. K., Grandi, G., and Rappuoli, R. (2006) Group B *Streptococcus:* global incidence and vaccine development. *Nat. Rev. Microbiol.* **4,** 932–942
2. Maione, D., Margarit, I., Rinaudo, C. D., Masignani, V., Mora, M., Scarselli, M., Tettelin, H., Brettoni, C., Iacobini, E. T., Rosini, R., D'Agostino, N., Miorin, L., Buccato, S., Mariani, M., Galli, G., Nogarotto, R., Dei, V. N., Vegni, F., Fraser, C., Mancuso, G., Teti, G., Madoff, L. C., Paoletti, L. C., Rappuoli, R., Kasper, D. L., Telford, J. L., and Grandi, G. (2005) Identification of a universal group B *Streptococcus* vaccine by multiple genome screen. *Science* **309,** 148–150
3. Margarit, I., Rinaudo, C. D., Galeotti, C. L., Maione, D., Ghezzo, C., Buttazzoni, E., Rosini, R., Runci, Y., Mora, M., Buccato, S.,

Pagani, M., Tresoldi, E., Berardi, A., Creti, R., Baker, C. J., Telford, J. L., and Grandi, G. (2009) Preventing bacterial infections with pilus-based vaccines: the group B *Streptococcus* paradigm. *J. Infect. Dis.* **199,** 108–115
4. Ton-That, H., Marraffini, L. A., and Schneewind, O. (2004) Protein sorting to the cell wall envelope of gram-positive bacteria. *Biochim. Biophys. Acta* **1694,** 269–278
5. Mandlik, A., Swierczynski, A., Das, A., and Ton-That, H. (2008) Pili in gram-positive bacteria: assembly, involvement in colonization and biofilm development. *Trends Microbiol.* **16,** 33–40
6. Telford, J. L., Barocchi, M. A., Margarit, I., Rappuoli, R., and Grandi, G. (2006) Pili in gram-positive pathogens. *Nat. Rev. Microbiol.* **4,** 509–519
7. Ton-That, H., Marraffini, L. A., and Schneewind, O. (2004) Sortases and pilin elements involved in pilus assembly of *Corynebacterium diphtheriae*. *Mol. Microbiol.* **53,** 251–261
8. Ton-That, H., Mazmanian, S. K., Faull, K. F., and Schneewind, O. (2000) Anchoring of surface proteins to the cell wall of *Staphylococcus aureus*. Sortase catalyzed in vitro transpeptidation reaction using LPXTG peptide and NH(2)-Gly(3) substrates. *J. Biol. Chem.* **275,** 9876–9881
9. Marraffini, L. A., Dedent, A. C., and Schneewind, O. (2006) Sortases and the art of anchoring proteins to the envelopes of gram-positive bacteria. *Microbiol. Mol. Biol. Rev.* **70,** 192–221
10. Lauer, P., Rinaudo, C. D., Soriani, M., Margarit, I., Maione, D., Rosini, R., Taddei, A. R., Mora, M., Rappuoli, R., Grandi, G., and Telford, J. L. (2005) Genome analysis reveals pili in group B *Streptococcus*. *Science* **309,** 105
11. Rosini, R., Rinaudo, C. D., Soriani, M., Lauer, P., Mora, M., Maione, D., Taddei, A., Santi, I., Ghezzo, C., Brettoni, C., Buccato, S., Margarit, I., Grandi, G., and Telford, J. L. (2006) Identification of novel genomic islands coding for antigenic pilus-like structures in *Streptococcus agalactiae*. *Mol. Microbiol.* **61,** 126–141
12. Nobbs, A. H., Rosini, R., Rinaudo, C. D., Maione, D., Grandi, G., and Telford, J. L. (2008) Sortase A utilizes an ancillary protein anchor for efficient cell wall anchoring of pili in *Streptococcus agalactiae*. *Infect. Immun.* **76,** 3550–3560
13. Lalioui, L., Pellegrini, E., Dramsi, S., Baptista, M., Bourgeois, N., Doucet-Populaire, F., Rusniok, C., Zouine, M., Glaser, P., Kunst, F., Poyart, C., and Trieu-Cuot, P. (2005) The SrtA Sortase of *Streptococcus agalactiae* is required for cell wall anchoring of proteins containing the LPXTG motif, for adhesion to epithelial cells, and for colonization of the mouse intestine. *Infect. Immun.* **73,** 3342–3350
14. Manzano, C., Contreras-Martel, C., El Mortaji, L., Izore, T., Fenel, D., Vernet, T., Schoehn, G., Di Guilmi, A. M., and Dessen, A. (2008) Sortase-mediated pilus fiber biogenesis in *Streptococcus pneumoniae*. *Structure* **16,** 1838–1848
15. Neiers, F., Madhurantakam, C., Falker, S., Manzano, C., Dessen, A., Normark, S., Henriques-Normark, B., and Achour, A. (2009) Two crystal structures of pneumococcal pilus sortase C provide novel insights into catalysis and substrate specificity. *J. Mol. Biol.* **393,** 704–716
16. Zong, Y., Bice, T. W., Ton-That, H., Schneewind, O., and Narayana, S. V. (2004) Crystal structures of *Staphylococcus aureus* sortase A and its substrate complex. *J. Biol. Chem.* **279,** 31383–31389
17. Zong, Y., Mazmanian, S. K., Schneewind, O., and Narayana, S. V. (2004) The structure of sortase B, a cysteine transpeptidase that tethers surface protein to the *Staphylococcus aureus* cell wall. *Structure* **12,** 105–112
18. Weiner, E. M., Robson, S. A., Marohn, M., and Clubb, R. T. The sortase A enzyme that attaches proteins to the cell wall of *B. anthracis* contains an unusual active site architecture. *J. Biol. Chem.*
19. Klock, H. E., and Lesley, S. A. (2009) The polymerase incomplete primer extension (PIPE) method applied to high-throughput cloning and site-directed mutagenesis. *Methods Mol. Biol.* **498,** 91–103
20. Otwinowski, Z., Borek, D., Majewski, W., and Minor, W. (2003) Multiparametric scaling of diffraction intensities. *Acta Crystallogr. A* **59,** 228–234
21. Collaborative Computational Project Number 4. (1994) The CCP4 suite: programs for protein crystallography. *Acta Crystallogr. D* **50,** 760–763
22. McCoy, A. J., Grosse-Kunstleve, R. W., Adams, P. D., Winn, M. D., Storoni, L. C., and Read, R. J. (2007) Phaser crystallographic software. *J. Appl. Crystallogr.* **40,** 658–674
23. Adams, P. D., Afonine, P. V., Bunkoczi, G., Chen, V. B., Davis, I. W., Echols, N., Headd, J. J., Hung, L. W., Kapral, G. J., Grosse-Kunstleve, R. W., McCoy, A. J., Moriarty, N. W., Oeffner, R., Read, R. J., Richardson, D. C., Richardson, J. S., Terwilliger, T. C., and Zwart, P. H. PHENIX: a comprehensive Python-based system for macromolecular structure solution. *Acta Crystallogr. D Biol. Crystallogr.* **66**, 213–221
24. Emsley, P., and Cowtan, K. (2004) Coot: model-building tools for molecular graphics. *Acta Crystallogr. D. Biol. Crystallogr.* **60,** 2126–2132
25. Laskowski, R. A., Moss, D. S., and Thornton, J. M. (1993) Main-chain bond lengths and bond angles in protein structures. *J. Mol. Biol.* **231,** 1049–1067
26. DeLano, W. (2002) *Pymol Molecular Graphics System*, De Lano Scientific, San Carlos, CA, USA
27. Wirth, R., An, F. Y., and Clewell, D. B. (1986) Highly efficient protoplast transformation system for *Streptococcus faecalis* and a new *Escherichia coli-S. faecalis* shuttle vector. *J. Bacteriol.* **165,** 831–836
28. Kling, D. E., Madoff, L. C., and Michel, J. L. (1999) Subcellular fractionation of group B *Streptococcus*. *BioTechniques* **27**, 24–26, 28
29. Buccato, S., Maione, D., Rinaudo, C. D., Volpini, G., Taddei, A. R., Rosini, R., Telford, J. L., Grandi, G., and Margarit, I. (2006) Use of *Lactococcus lactis* expressing pili from group B *Streptococcus* as a broad-coverage vaccine against streptococcal disease. *J. Infect. Dis.* **194,** 331–340
30. Rinaudo, C. D., Rosini, R., Galeotti, C. L., Berti, F., Necchi, F., Reguzzi, V., Ghezzo, C., Telford, J. L., Grandi, G., and Maione, D. Specific involvement of pilus type 2a in biofilm formation in group B *Streptococcus*. *PLoS One* 5, e9216
31. Viguera, A. R., and Serrano, L. (1995) Side-chain interactions between sulfur-containing amino acids and phenylalanine in alpha-helices. *Biochemistry* **34,** 8771–8779
32. Van Stipdonk, M. J., Badia-Martinez, D., Sluijter, M., Offringa, R., van Hall, T., and Achour, A. (2009) Design of agonistic altered peptides for the robust induction of CTL directed towards H-2Db in complex with the melanoma-associated epitope gp100. *Cancer Res.* **69,** 7784–7792
33. Brandl, M., Weiss, M. S., Jabs, A., Suhnel, J., and Hilgenfeld, R. (2001) C-H.pi-interactions in proteins. *J. Mol. Biol.* **307,** 357–377
34. Manzano, C., Izore, T., Job, V., Di Guilmi, A. M., and Dessen, A. (2009) Sortase activity is controlled by a flexible lid in the pilus biogenesis mechanism of gram-positive pathogens. *Biochemistry* **48,** 10549–10557
35. Naik, M. T., Suree, N., Ilangovan, U., Liew, C. K., Thieu, W., Campbell, D. O., Clemens, J. J., Jung, M. E., and Clubb, R. T. (2006) *Staphylococcus aureus* sortase A transpeptidase. Calcium promotes sorting signal binding by altering the mobility and structure of an active site loop. *J. Biol. Chem.* **281,** 1817–1826
36. Holm, L., Kaariainen, S., Rosenstrom, P., and Schenkel, A. (2008) Searching protein structure databases with DaliLite v. 3. *Bioinformatics* **24,** 2780–2781
37. Huang, X., Aulabaugh, A., Ding, W., Kapoor, B., Alksne, L., Tabei, K., and Ellestad, G. (2003) Kinetic mechanism of *Staphylococcus aureus* sortase SrtA. *Biochemistry* **42,** 11307–11315
38. Dramsi, S., Trieu-Cuot, P., and Bierne, H. (2005) Sorting sortases: a nomenclature proposal for the various sortases of gram-positive bacteria. *Res. Microbiol.* **156,** 289–297
39. Pallen, M. J., Lam, A. C., Antonio, M., and Dunbar, K. (2001) An embarrassment of sortases—a richness of substrates? *Trends Microbiol.* **9,** 97–102
40. Ilangovan, U., Ton-That, H., Iwahara, J., Schneewind, O., and Clubb, R. T. (2001) Structure of sortase, the transpeptidase that anchors proteins to the cell wall of *Staphylococcus aureus*. *Proc. Natl. Acad. Sci. U. S. A.* **98,** 6056–6061
41. Landau, M., Mayrose, I., Rosenberg, Y., Glaser, F., Martz, E., Pupko, T., and Ben-Tal, N. (2005) ConSurf 2005: the projection of evolutionary conservation scores of residues on protein structures. *Nucleic Acids Res.* **33,** W299–302
42. Nakata, M., Koller, T., Moritz, K., Ribardo, D., Jonas, L., McIver, K. S., Sumitomo, T., Terao, Y., Kawabata, S., Podbielski, A., and Kreikemeyer, B. (2009) Mode of expression and functional characterization of FCT-3 pilus region-encoded proteins in *Streptococcus pyogenes* serotype M49. *Infect. Immun.* **77,** 32–44
43. Guttilla, I. K., Gaspar, A. H., Swierczynski, A., Swaminathan, A., Dwivedi, P., Das, A., and Ton-That, H. (2009) Acyl enzyme intermediates in sortase-catalyzed pilus morphogenesis in gram-positive bacteria. *J. Bacteriol.* **191,** 5603–5612

Received for publication October 28, 2010.
Accepted for publication February 10, 2011.